Atmos. Chem. Phys. Discuss., doi:10.5194/acp-2016-490, 2016
Manuscript under review for journal Atmos. Chem. Phys.
Published: 20 June 2016

Atmospheric Chemistry and Physics Discussions

Investigating Wavelength-Dependent Aerosol Optical Properties Using Water Vapor Slant Column Retrievals from CLARS over the Los Angeles Basin

Zhao-Cheng Zeng[1,2], Qiong Zhang[1], Jack S. Margolis[3], Run-Lie Shia[1], Sally Newman[1], Dejian Fu[4], Thomas J. Pongetti[4], Kam W. Wong[1,4], Stanley P. Sander[4], Paul O. Wennberg[1] and Yuk L. Yung[1]

[1]Division of Geological and Planetary Sciences, California Institute of Technology, Pasadena, CA 91125, USA
[2]Institute of Space and Earth Information Science, The Chinese University of Hong Kong, Hong Kong, China
[3]1842 Rose Villa St., Pasadena, CA 91107, USA
[4]Jet Propulsion Laboratory, California Institute of Technology, Pasadena, CA 91109, USA

Correspondence to: Zhao-Cheng Zeng (zcz@gps.caltech.edu)

Abstract. In this study, we propose a novel approach to constrain the optical properties of atmospheric aerosol in a complex urban environment using water vapor (H_2O) slant column measurements in the near infrared. This approach is demonstrated using measurements from the California Laboratory for Atmospheric Remote Sensing Fourier Transform Spectrometer (CLARS-FTS) on the top of Mt. Wilson, California, and a two-stream-exact single scattering (2S-ESS) radiative transfer (RT) model. From the spectral measurements, we retrieve H_2O slant column density (SCD) using 15 different absorption bands between 4000 and 8000 cm^{-1}. Due to the wavelength dependence of aerosol scattering, large variations in H_2O SCD retrievals are observed as a function of wavelength. Moreover, the variations are found to be correlated with aerosol optical depths (AOD) measured at the AERONET-Caltech station. Simulation results from the RT model reproduce this correlation and show that the aerosol scattering is the primary contributor to the variations in the wavelength dependence of the H_2O SCD retrievals. The evidence from both measurements and simulations suggest that wavelength-dependent aerosol optical properties can be constrained using H_2O retrievals from multiple bands.

1 Introduction

Greenhouse gas (GHG) observations from space provide unprecedented global measurements of column GHG concentration, facilitating inference of the carbon fluxes on regional scales (Yoshida et al., 2011; Crisp et al., 2012). However, atmospheric aerosol scattering has been shown to have a considerable impact on the retrieval of GHGs from space-based observations in the near infrared (Aben et al., 2007; Yoshida et al., 2011; O'Dell et al., 2012). A study by O'Dell et al. (2012) showed that the error budget in the satellite retrievals of column-averaged dry-air mole fraction of CO_2 (XCO_2) is dominated by systematic errors due to imperfect characterization of clouds and aerosol properties. Previous studies also showed that by incorporating simple aerosol properties into the retrieval state variables, the bias can be greatly mitigated (Butz et al., 2009; Guerlet et al., 2013). It is therefore crucial to characterize the aerosol properties for the retrieval algorithm of GHGs.

Atmos. Chem. Phys. Discuss., doi:10.5194/acp-2016-490, 2016
Manuscript under review for journal Atmos. Chem. Phys.
Published: 20 June 2016

Atmospheric Chemistry and Physics Discussions

However, aerosols have complex types and size distributions and are highly variable in density. Their optical properties are very hard to measure directly (Seinfeld and Pandis, 2006). The global ground-based aerosol monitoring network, AERONET (Holben et al., 1998), has been providing high-accuracy measurements of total AOD from ultraviolet to near infrared spectral region, but is sparsely distributed, suggesting that it would be useful to have further means of constraining aerosol optical properties.

Water vapor has absorption features across the electromagnetic spectrum, from the ultraviolet to the infrared. In a non-scattering atmosphere, H_2O retrievals from different absorption bands would give exactly the same value. However, due to the wavelength-dependent aerosol scattering (Eck et al., 1999; Zhang et al., 2015), the different light path changes in different absorption bands result in discrepancies in H_2O retrievals. This variation in H_2O retrievals from different bands can therefore provide information on aerosol properties. Based on this theory, we here propose a novel approach to constrain the aerosol properties, mainly aerosol optical depth (AOD), using the variation in H_2O retrievals from multiple bands. This approach is illustrated with data from The California Laboratory for Atmospheric Remote Sensing (CLARS), which continuously collects high-resolution spectra in the near infrared. A two-stream enhanced single scattering (2S-ESS) radiative transfer (RT) model is used to simulate the observations and explain the physical mechanism behind the proposed approach. The additional information on aerosol optical properties gained by applying this approach could be used to improve retrievals of GHGs from space in the presence of aerosols.

In section 2, a detailed description of the CLARS-FTS is presented. Section 3 introduces the 15 different bands chosen for retrieving H_2O from CLARS measurements. In section 4, the correlation between variations in H_2O retrievals from different bands and AOD data from AERONET-Caltech is discussed. In section 5, the dominant causation of aerosol scattering on the variations in H_2O retrievals is illustrated using the 2S-ESS RT model. Discussion and conclusions are presented in section 6 and 7, respectively.

2 CLARS

The CLARS-FTS is located near the top of Mt. Wilson at an altitude of 1670 m a.s.l. overlooking 28 land target sites in Los Angeles (Supplemental material Table 1 and Figure 1 of Fu et al., 2014; Wong et al., 2015). It offers continuous high-resolution spectral measurements from 4000 to 8000 cm^{-1}. As shown in Figure 1, CLARS-FTS has two operation modes: the Spectralon Viewing Observation (SVO) mode and the Los Angeles Basin Surveys (LABS) mode. In SVO mode, the FTS looks at a Spectralon® plate adjacent to the FTS to observe the reflected solar spectrum from the free troposphere above Mt. Wilson, which is usually above the planetary boundary layer (PBL) and relatively immune to aerosol scattering. In LABS, the FTS looks down at target sites in the LA basin to observe the reflected sunlight, which travels through a long light path within the urban PBL (Figure 1) and undergoes absorption and scattering by gas molecules and aerosols. This observation geometry by LABS mode makes CLARS-FTS measurements not only highly sensitive to the atmospheric composition in the

Atmos. Chem. Phys. Discuss., doi:10.5194/acp-2016-490, 2016
Manuscript under review for journal Atmos. Chem. Phys.
Published: 20 June 2016

PBL but also very susceptible to influence by aerosol scattering and absorption. This CLARS measurement technique from Mount Wilson mimics geostationary satellite observations of reflected sunlight and measures atmospheric absorptions by GHGs along the optical paths, including the incident path from the sun to the surface and the reflection path from the surface to the instrument (Xi et al., 2015).

Slant column density (SCD), the total number of absorbing molecules per unit area along the optical path, is retrieved for H_2O using the version 1.0 operational retrieval algorithm of CLARS-FTS (Fu et al., 2014), developed based on the Gas Fitting tool (GFIT) algorithm that has been widely used for the Total Carbon Column Observing Network (TCCON) network (Toon et al., 1992; Wunch et al., 2011). Surface reflection is included in the modified version but aerosol scattering is not taken into account. Thus, errors in the SCD retrieval are largely due to light path changes caused by aerosol scattering, and can be used as a proxy for aerosol loading. It is worth noting that the major impacts of aerosol scatterings on CLARS-FTS operational data productions of XCO_2, XCH_4, and XCO have been removed. Collocated O_2 measurements were retrieved from the 1.27-um band and were used as a proxy for light path calibration (Fu et al., 2014; Wong et al., 2015; Wong et al., 2016). A detailed description of the observation system of CLARS-FTS, measurement sequence, operational retrieval algorithms and characteristics of operational data products can be found in Fu et al. (2014). The 15 different bands used in this study for retrieving H_2O SCDs from CLARS-FTS are introduced in Section 3.

3 Bands for H_2O retrievals

H_2O has absorption features across the electromagnetic spectrum including many absorption lines in the near infrared as well as significant continuum absorption. Within the spectral range of CLARS-FTS observations, we carefully select 15 spectral intervals containing H_2O absorption lines, as shown in Figure 2, across the spectral range from 4000 to 8000 cm^{-1} for retrieving H_2O SCD. Each interval is 5 to 14 cm^{-1} wide and contains 2 to 9 moderately strong absorption lines. Rodgers (2000) showed that information analysis is a powerful tool for evaluating the efficiency of band channels selected for retrieval. Therefore, we conduct information analysis by calculating the information content (IC) for each band selected for retrieving H_2O SCD. A detailed theoretical description of the information analysis can be found in Su et al. (2015). The radiative transfer model used here is the numerically efficient 2S-ESS RT model (Spurr and Natraj, 2011). The detailed settings of 2S-ESS are described in Section 5. Here, we assume that only one state variable, i.e., H_2O SCD, is retrieved. Therefore, the information content values shown in Figure 2 are for H_2O retrieval only. They reflect the precision of H_2O retrieval in each selected band. For any band with IC value equal to x, as many as e^x different atmospheric H_2O states can be distinguished (Rodgers, 2000). The purpose of the IC calculation is to show the sensitivity of each absorption band to the variation of H_2O SCD. While fitting the CLARS-FTS measured spectra, we retrieve more state variables including other trace gas abundances and continuum shape parameters (Fu et al., 2014). From the IC results shown in Figure 2, we can see that the average IC is high (about 6 on average) and similar among all bands, which indicates very high retrieval precision

Atmos. Chem. Phys. Discuss., doi:10.5194/acp-2016-490, 2016
Manuscript under review for journal Atmos. Chem. Phys.
Published: 20 June 2016

Atmospheric Chemistry and Physics Discussions

compared with the *a priori* information (Rogers, 2000). H_2O SCDs retrieved from these 15 bands will be shown in the following section.

4 H_2O SCD retrievals from CLARS and its correlation with aerosol optical depth

4.1 Daily variation

Figure 3 shows examples of daily CLARS H_2O SCD retrievals on March 01, 2013 and September 28, 2013. On these two days, there were dense observations for the West Pasadena target retrieved using the 15 bands shown in Figure 2. In particular, we compare retrievals from SVO (Figure 3(a)), which is above the PBL (Newman et al., 2013) and therefore relatively unaffected by aerosol scattering, with those from the West Pasadena target (Figure 3(b)), a location in the Los Angeles basin that is influenced by aerosol scattering. The H_2O SCD retrievals from SVO are nearly identical across different wavelengths, and the small differences may be attributed to the band-to-band inconsistency of line parameters. However, H_2O SCD retrievals for West Pasadena show significantly larger variation across different wavelengths. These retrieval differences are much larger than those attributed to spectroscopic uncertainties, and reflect the wavelength dependence of aerosol scattering in the boundary layer. To quantify the variation in the H_2O SCD retrievals from the 15 bands, the standard deviation (σ) of the retrievals is calculated by,

$$\sigma = \sqrt{\sum_{i=1}^{n}[(s_i - \bar{s})^2]/(n-1)}, \quad (1)$$

where n=15 is the number of bands, s_i is the SCD retrieval for band i, and $\bar{s} = (\sum_{i=1}^{n} s_i)/n$ is the mean. The standard deviations in Figure 3 (c) show that the variations in H_2O SCD retrievals monotonically increase throughout the day. As shown in Figure 3 (d), the AOD data on these two days from AERONET-Caltech shows a typical pattern for the LA basin. AOD increases from the morning to the afternoon. Note here that the AERONET station measures mainly in the visible wavelengths from 340 to 1020 nm. However, we assume they are also good proxies for AOD in the near infrared. The increasing trend of AOD corresponds well to that of the standard deviations of H_2O SCD retrievals. This correlation from daily measurements shows the potential of constraining the AOD using the standard deviation of H_2O SCD retrievals. However, apart from aerosol scattering, the daily variation of standard deviations of H_2O SCD retrievals can also be influenced by differences in observation geometry, such as solar zenith angle (SZA) and relative azimuth angle (AZA), variations in planetary boundary layer height (PBLH) and changes in spatial distribution of aerosol. All of these parameters are changing during the day.

4.2 Seasonal variation

To quantitatively compare the variations in H_2O SCD retrievals and AOD, we choose the daily mean of the data between 12:00 and 14:00 local time when there is generally less haze or fog. This time is also coincident with the local crossing time of the two currently operating greenhouse gas observation satellites, GOSAT (Yoshida et al., 2011) and OCO-2 (Crisp et al.,

Atmos. Chem. Phys. Discuss., doi:10.5194/acp-2016-490, 2016
Manuscript under review for journal Atmos. Chem. Phys.
Published: 20 June 2016

Atmospheric Chemistry and Physics Discussions

2012). We focus on a two-hour period to limit the effect of other parameters on the H_2O retrieval standard deviation, such as solar geometry and PBLH. The concurrent AOD data for CLARS retrievals are chosen to be the closest AERONET AOD data. If their measurement time difference is more than 30 min, then the CLARS data are not used. AERONET-Caltech has AOD measurements in seven wavelengths from 340 to 1020 nm, and we choose the data at 1020 nm, which is the closest to the wavelengths for retrieving H_2O in this study. Furthermore, the AOD data are scaled to be the optical depths along the slant path, which is the aerosol optical path (AOP), according to the SZA and viewing zenith angle of CLARS at West Pasadena (83.1 °). As a result, in total 67 daily mean data pairs are available in 2013 after excluding days (1) that are cloudy according to the images from the visible camera looking at the target and (2) in which there are fewer than 3 valid observations. We separate the data into two different time periods, the winter-spring season (December, and January to May) and the summer-autumn season (June to November) by considering the different dominant wind directions between winter and summer in Pasadena (Conil and Hall, 2006; Newman et al. 2016). In summer the prevailing winds come from the southwest across the basin; and in winter the winds come from the northeast across the mountains and deserts. Different wind patterns suggest that the dominant aerosol types in these two time periods may be different (Newman et al., 2013). Also for each of these two time periods, we expect the CLARS observation geometry and PBLH at noon time to be similar across the days, and therefore assume their effects on H_2O retrievals to be similar. In fact, from the RT model simulation in Section 5 we can see that the contributions to the variation in H_2O retrievals from other factors are actually much smaller than those from aerosol scattering, even though the geometry and PBLH change a lot during a day.

Figure 4 shows significant linear correlations between the AOP value and standard deviation of H_2O SCDs for the two time periods, both with R^2 around 0.5. However, the slopes from linear regression between AOP and the standard deviation of H_2O SCD retrievals are different. In summer-autumn, the regression slope, an indication of the degree of light path change due to aerosol scattering relative to change of aerosol loading, is about one half of that in winter-spring, indicating that for the same AOD, the variation in H_2O SCD retrievals in summer-autumn is about twice that in winter-spring. This may be due to the different size distributions and scattering phase functions of aerosols in these two time periods. In addition, H_2O abundance shows significant seasonal variation in the LA basin, and previous studies have shown, for example, that aerosol optical properties change dramatically with relative humidity (e.g. Thompson et al., 2012).

5 Simulations by two-stream radiative transfer model

In this section, we use a radiative transfer (RT) model to simulate the measurements, explain the cause, and quantify the role of aerosol scattering in the variation in H_2O SCDs from CLARS. The model is a numerically efficient 2S-ESS RT model (Spurr and Natraj, 2011), in which the single scattering radiation is computed exactly while the multiply-scattered radiation is calculated using the two-stream approximation. It has been used to study the remote sensing of GHGs in several previous studies (Xi et al., 2015; Zhang et al., 2015; Zhang et al., 2016).

Atmos. Chem. Phys. Discuss., doi:10.5194/acp-2016-490, 2016
Manuscript under review for journal Atmos. Chem. Phys.
Published: 20 June 2016

Atmospheric Chemistry and Physics Discussions

With this 2S-ESS RT model, we simulate the spectral radiance observed by CLARS-FTS for the West Pasadena target. The settings of this model are largely the same as those used by Zhang et al. (2015). Some essential settings and modifications are as follows. In this RT model, (1) the a priori atmospheric profile is obtained from National Centers for Environmental Prediction (NCEP)-National Center for Atmospheric Research (NCAR) reanalysis data (Kalnay et al., 1996). The profile has 70 layers from the surface up to 70 km; (2) absorption coefficients for all absorbing gas molecules are derived from the HITRAN version 2008 database (Rothman et al., 2009); (3) the optical depth for each layer is calculated using the Reference Forward Model (Dudhia et al., 2002); (4) the surface reflection is assumed to be Lambertian with a surface albedo of 0.23, measured by Fu et al. (2014) for West Pasadena; (5) Rayleigh scattering by air molecules is considered in this RT model; (6) the observation geometry, including the viewing zenith angle for the West Pasadena target, the daily solar zenith angle (SZA), and the relative azimuth angle (AZA) on March 01, 2013 are included in the model; (7) the aerosol scattering phase function in the model is assumed to follow the Henyey-Greenstein type phase function (Henyey and Greenstein, 1941). Climatologic aerosol compositions for 5 types of aerosol (black carbon, organic carbon, sulfate, coarse, and accumulation mode sea salt) and size distributions are obtained from modeling (Zhang et al., 2015). The aerosol optical properties (single scattering albedo and asymmetry factor) are calculated as described in Zhang et al. (2015). A detailed description of the typical aerosol composition and optical parameters in LA is shown in Table 1 of Zhang et al. (2015); (8) unlike Zhang et al. (2015), in this study, the average hourly PBLH data measured over late spring in 2010 in LA (Newman et al., 2013) are used. Unlike CO_2, H_2O mixing ratio varies dramatically with altitude across the total column atmosphere (Seinfeld and Pandis, 2006). In the LA basin, a large portion of H_2O is concentrated within the PBL. Therefore, the PBLH is an important parameter in modeling the effect of scattering on the H_2O retrieval. The model output radiance is convolved using the CLARS-FTS instrument line shape with full width at half maximum (FWHM) = 0.022cm^{-1} (Fu et al., 2014). The spectral resolution is set to be 0.06 cm^{-1}, and the corresponding instrument maximum optical path difference is 5.0 cm. The signal-to-noise ratio is assumed to be constant at 300. We perturb the simulated spectra with Gaussian white noise.

The wavelength range covered by AERONET-Caltech measurements is from 340 to 1020 nm; however, the H_2O absorption bands used in this study are not included. To calculate the AOD in these 15 bands, we use the Ångström exponent law to extrapolate the data (Seinfeld and Pandis, 2006; Zhang et al., 2015). The extrapolated AOD data on March 01, 2013 for the 15 bands are included in the RT model, assuming non-zero AOD is evenly distributed vertically and horizontally in the PBL.

In order to quantify the influence of aerosol scattering on the H_2O SCD retrievals, we simulate the bias observed by CLARS-FTS by (1) using the 2S-ESS RT model to generate synthetic spectral radiance data for the 15 chosen bands, and (2) fitting the synthesis spectra data and retrieve H_2O SCD based on the Bayesian inversion theory (Rodgers, 2000) using the forward 2S-ESS RT model with the same configuration, but with AOD set to zero and held constant, as in Zhang et al. (2015). This approach approximately simulates the influence of neglecting aerosol scattering on the retrieved H_2O SCDs by CLARS. The fitting process employs the Levenberg-Marquardt algorithm (Rodgers, 2000). The state vector element to be retrieved from

Atmos. Chem. Phys. Discuss., doi:10.5194/acp-2016-490, 2016
Manuscript under review for journal Atmos. Chem. Phys.
Published: 20 June 2016

the inversion approach is the scaling factor, which is the ratio of retrieved H_2O SCD to the assumed "truth" data in the model from NCEP reanalysis data. Two experiments are compared to demonstrate the effect of aerosol scattering on the variations in H_2O SCD retrievals. In the first experiment, the AOD data vary during the day in the same way as the AERONET-Caltech measurements, while in the second, control, experiment, the AOD data are fixed at the 8:00 am level for all hours across the day. The results of simulated H_2O SCD retrieval scaling factors are shown in Figure 5(a) and (b) for these two experiments, respectively. The scaling factors (f) are mean-centered by subtracting the mean to clearly show the variations in the data. The mean-centered scaling factor is calculated by, $\hat{f}_i = f_i - \bar{f}$ for i = 1 to 15, where f_i is the scaling factor and $\hat{f}_i$ is the mean-centering scaling factor for band i, and $\bar{f}$ is the mean of the scaling factors. From Figure 5(a), we can see that the variation in the simulated H_2O SCD retrievals increases with the increasing AOD from the morning to the afternoon, the same as we see from the CLARS observations in Figure 3(b) and (c). However, since the results from the control experiment show much smaller diurnal change of variation, as shown in Figure 5(b), than the first experiment, aerosol scattering must be the dominant cause of the variations in H_2O SCD retrievals. Further confirmation of this is demonstrated in Figure 5(c), which shows the comparison between CLARS measurements and the two RT model experiments in terms of normalized standard deviation of H_2O SCDs. As with the CLARS measurements, the standard deviations of the scaling factors are calculated using equation (1). To focus on comparison of relative change in variations of H_2O SCDs between measurements and simulations, their standard deviations (σ) are normalized to be between 0 and 1. The normalized standard deviations are calculated as $\tilde{\sigma}_t = (\sigma_t - \sigma_{min})/(\sigma_{max} - \sigma_{min})$, where σ_t is the standard deviation and $\tilde{\sigma}_t$ is the normalized standard deviation at time t, and σ_{max} and σ_{min} are maximum and minimum standard deviations, respectively, across the day. This normalization is independently implemented for measurements and simulations. When normalizing the CLARS measurements, the half-hourly means of the data are calculated to obtain the maximum and minimum. From Figure 5(c), we can see that the increasing trend from measurements is very similar to that from the simulations from the first experiment, while the trend is much smaller for the control experiment. The major difference between them can be attributed to the effect of aerosol scattering in the PBL. From this RT model simulation, we conclude that aerosol scattering is the dominant factor contributing to the variations in H_2O SCD retrievals, and the correlation between AOD and standard deviations of H_2O SCD retrievals from measurements is robust. Therefore, the H_2O SCD retrievals from CLARS show its potential in constraining the aerosol properties in the LA basin.

6 Discussion

6.1 Assumptions

When comparing the H_2O SCD retrievals from CLARS for the West Pasadena target with AOD data from AERONET-Caltech in Figures 3 and 4, two assumptions are made: (1) we assume homogeneous aerosol distribution between West Pasadena and Caltech. Since the distance between them is 5 km, which is small in terms of the whole LA basin, we would

Atmos. Chem. Phys. Discuss., doi:10.5194/acp-2016-490, 2016
Manuscript under review for journal Atmos. Chem. Phys.
Published: 20 June 2016

expect the AOD variation at Caltech represents that in West Pasadena well. However, local topography is complex and the AOD horizontal distribution can be inhomogeneous (Lu et al., 1994). The differences between these two locations may contribute to the scatter of data and slightly lower R^2 in Figure 4(b) compared to Figure 4(a); (2) we assume, in Figure 4, that the changes of CLARS observation geometry and PBLH at noon across the days in 2013 within either winter-spring or summer-autumn are small, as well as their effects on the variations in H_2O SCD retrievals from multiple bands. This assumption is supported by the results from RT modeling that contributions from factors other than AOD are very small even though the diurnal variations in observation geometry and PBLH are large.

6.2 Limitations

There are some limitations of the approach outlined here. First, in the 2S-ESS RT model, we use the climatologic aerosol types and size distributions in LA because of the lack of temporal resolution measurements of the aerosol properties in this region. In the future, more cases with different compositions of aerosol should be incorporated into the RT model to explore this proposed approach. Second, due to the limited number of concurrent observations of H_2O SCD and AOD, the correlation is only explored in two different time periods in 2013, the winter-spring seasons and summer-autumn seasons. Ideally correlation between the two data sets in smaller time intervals can provide more detailed information of the aerosol properties. Finally, the CLARS data are explored for the West Pasadena target only since this location is closest to the AERONET-Caltech station, which is regarded as the ground-truth. More data from other targets of CLARS may be explored in the future.

7 Conclusions

We illustrate the robust ability of multi-wavelength retrievals of water vapor slant columns to provide constraints on aerosol optical properties. We apply this approach to the H_2O SCD retrievals from 15 different absorption bands using spectral data observed by CLARS-FTS. We explore the correlation between the variation in H_2O SCDs and the concurrent AOD data observed by AERONET-Caltech, and further use the 2S-ESS RT model to quantitatively demonstrate the dominant role of aerosol scattering in the variation in H_2O SCD data and justify the potential of using H_2O retrievals in constraining aerosol properties. We find: (1) The wavelength dependence of aerosol scattering can be clearly observed by comparing the CLARS H_2O SCD retrievals between SVO and LABS modes; (2) A significant linear correlation is found between the standard deviations of H_2O SCDs and AOD data. Results from RT modeling are consistent with the observations demonstrating that aerosol scattering is the dominant cause of the variation in H_2O SCDs. These two pieces of evidence justify our proposed approach to constrain aerosol properties using H_2O retrievals, providing a sensitive way to quantify the effect of aerosol scattering in GHGs retrievals and potentially contribute toward reducing errors of GHGs retrievals from space.

Atmos. Chem. Phys. Discuss., doi:10.5194/acp-2016-490, 2016
Manuscript under review for journal Atmos. Chem. Phys.
Published: 20 June 2016

Atmospheric Chemistry and Physics Discussions

Acknowledgments

We thank M. Gunson and A. Eldering for stimulating discussions and support, V. Natraj for providing the 2S-ESS radiative transfer code, and M. Gerstell for proofreading the manuscript. Part of the research in this study was performed at the Jet Propulsion Laboratory (JPL), California Institute of Technology (Caltech), under a contract with the National Aeronautics and Space Administration (NASA). Support from the Caltech KISS Megacity project, the NIST GHG and Climate Science Program and NASA's Carbon Cycle Science Program through the JPL is gratefully acknowledged. Z.-C. Zeng was supported by a postgraduate studentship for overseas academic exchange from the Chinese University of Hong Kong. We thank Jochen Stutz and his staff for their effort in establishing and maintaining the AERONET Caltech site. The AERONET data for this paper can be downloaded online (http://aeronet.gsfc.nasa.gov); CLARS-FTS data are available from the authors upon request.

References

Aben, I., Hasekamp, O., and Hartmann, W.: Uncertainties in the space-based measurements of CO_2 columns due to scattering in the Earth's atmosphere, J. Quant. Spectrosc. Radiat. Transfer, 104, 450–459, doi:10.1016/j.jqsrt.2006.09.013, 2007.

Butz, A., Hasekamp, O. P., Frankenberg, C., and Aben, I.: Retrievals of atmospheric CO_2 from simulated space-borne measurements of backscattered near-infrared sunlight: accounting for aerosol effects, Appl. Optics, 48, 3322–3336, doi:10.1364/AO.48.003322, 2009.

Conil, S., and Hall, A.: Local regimes of atmospheric variability: A case study of southern California, J. Clim., 19, 4308–4325, doi:10.1175/JCLI3837.1, 2006.

Crisp, D., Fisher, B. M., O'Dell, C., Frankenberg, C., Basilio, R., Bösch, H., Brown, L. R., Castano, R., Connor, B., Deutscher, N. M., Eldering, A., Griffith, D., Gunson, M., Kuze, A., Mandrake, L., McDuffie, J., Messerschmidt, J., Miller, C. E., Morino, I., Natraj, V., Notholt, J., O'Brien, D. M., Oyafuso, F., Polonsky, I., Robinson, J., Salawitch, R., Sherlock, V., Smyth, M., Suto, H., Taylor, T. E., Thompson, D. R., Wennberg, P. O., Wunch, D., and Yung, Y. L.: The ACOS CO_2 retrieval algorithm – Part II: Global XCO2 data characterization, Atmos. Meas. Tech., 5, 687–707, doi:10.5194/amt-5-687-2012, 2012.

Dudhia, A., Morris, P. E., and Wells, R. J.: Fast monochromatic radiative transfer calculations for limb sounding, J. Quant. Spectrosc. Radiat. Transfer, 74(6), 745–756, doi:10.1016/S0022-4073(01)00285-0, 2002.

Eck, T. F., Holben, B. N., Reid, J. S., Dubovik, O., Smirnov, A., O'Neill, N. T., Slutsker, I., and Kinne, S.: Wavelength dependence of the optical depth of biomass burning, urban, and desert dust aerosols, J. Geophys. Res., 104, 31333–31349, 1999.

Fu, D., Pongetti, T. J., Blavier, J.-F. L., Crawford, T. J., Manatt, K. S., Toon, G. C.,Wong, K.W., and Sander, S. P.: Near-infrared remote sensing of Los Angeles trace gas distributions from a mountaintop site, Atmos. Meas. Tech., 7, 713–729, doi:10.5194/amt-7-713-2014, 2014.

Goody, R. M., and Yung, Y. L.: Atmospheric Radiation: Theoretical Basis, 2nd ed., Oxford Univ. Press, Oxford, U. K., 1989.

Guerlet, S., Butz, A., Schepers, D., Basu, S., Hasekamp, O. P., Kuze, A., Yokota, T., Blavier, J.-F., Deutscher, N. M., Griffith, D. W. T., Hase, F., Kyro, E., Morino, I., Sherlock, V., Sussmann, R., Galli, A., and Aben, I.: Impact of aerosol and thin cirrus on retrieving and validating XCO_2 from GOSAT shortwave infrared measurements, J. Geophys. Res.-Atmos., 118, 4887–4905, doi:10.1002/jgrd.50332, 2013.

Holben, B. N., Eck, T. F., Slutsker, I., Tanre, D., Buis, J. P., Setzer, A., Vermote, E., Reagan, J. A., Kaufman, Y., Nakajima, T., Lavenu, F., Jankowiak, I., and Smirnov, A.: AERONET-A federated instrument network and data archive for aerosol characterization, Remote Sens. Environ., 66, 1–16, 1998.

Kalnay, E., Kanamitsu, M., Kistler, R., Collins, W., Deaven, D., Gandin, L., Iredell, M., Saha, S., White, G., Woollen, J., Zhu, Y., Chelliah, M., Ebisuzaki, W., Higgins, W., Janowiak, J., Mo, K. C., Ropelewski, C., Wang, J., Leetmaa, A., Reynolds, R., Jenne, R., and Joseph, D.: The NCEP/NCAR 40-year reanalysis project, B. Am. Meteorol. Soc., 77, 437–471, 1996.

Lu, R. and Turco, R. P.: Air pollutant transport in a coastal environment. Part I. Two-dimensional simulations of sea-breeze and mountain effects, J. Atmos. Sci., 51, 2285–2308, 1994.

Newman, S., Jeong, S., Fischer, M. L., Xu, X., Haman, C. L., Lefer, B., Alvarez, S., Rappenglueck, B., Kort, E. A., Andrews, A. E., Peischl, J., Gurney, K. R., Miller, C. E., and Yung, Y. L.: Diurnal tracking of anthropogenic CO_2 emissions in the Los Angeles basin megacity during spring 2010, Atmos. Chem. Phys., 13, 4359–4372, doi:10.5194/acp-13-4359-2013, 2013.

O'Dell, C. W., Connor, B., Bösch, H., O'Brien, D., Frankenberg, C., Castano, R., Christi, M., Crisp, D., Eldering, A., Fisher, B., Gunson, M., McDuffie, J., Miller, C. E., Natraj, V., Oyafuso, F., Polonsky, I., Smyth, M., Taylor, T., Toon, G. C.,Wennberg, P. O., and Wunch, D.: The ACOS CO_2 retrieval algorithm – Part 1: Description and validation against synthetic observations, Atmos. Meas. Tech., 5, 99–121, doi:10.5194/amt-5-99-2012, 2012.

Rodgers, C. D.: Inverse Methods for Atmospheric Sounding: Theory and Practice, World Scientific, Singapore, 2000.

Rothman, L. S., Gordon, I. E., Barbe, A., Benner, D. C., Bernath, P. E., Birk, M., Boudon, V., Brown, L. R., Campargue, A., Champion, J. P., Chance, K., Coudert, L. H., Dana, V., Devi, V. M., Fally, S., Flaud, J. M., Gamache, R. R., Goldman, A., Jacquemart, D., Kleiner, I., Lacome, N., Lafferty, W. J., Mandin, J. Y., Massie, S. T., Mikhailenko, S. N., Miller, C. E., Moazzen-Ahmadi, N., Naumenko, O. V., Nikitin, A. V., Orphal, J., Perevalov, V. I., Perrin, A., Predoi-Cross, A., Rinsland, C. P., Rotger, M., Simeckova, M., Smith, M. A. H., Sung, K., Tashkun, S. A., Tennyson, J., Toth, R. A., Vandaele, A. C., and Vander Auwera, J.: The HITRAN 2008 molecular spectroscopic database, J. Quant. Spectrosc. Radiat. Transfer, 110, 533–572, doi:10.1016/j.jqsrt.2009.02.013, 2009.

Seinfeld, J. and Pandis, S.: Atmospheric chemistry and physics: from air pollution to climate change, Wiley, Inc., New Jersey, USA, p.1224, 2006.

Spurr, R., and Natraj, V.: A linearized two-stream radiative transfer code for fast approximation of multiple-scatter fields, J. Quant. Spectrosc. Radiat. Transfer, 112(16), 2630–2637, doi:10.1016/j.jqsrt.2011.06.014, 2011.

Su, Z., Xi, X., Natraj, V., Li, K.-F., Shia, R.-L., Miller, C. E., and Yung, Y. L.: Information-rich spectral channels for simulated retrievals of partial column-averaged methane, Earth Space Sci., 3, 2-14, doi:10.1002/2015EA000120, 2016.

Thompson, J.E., Hayes, P.L., Jimenez, J.L., Adachi, K., Zhang, X., Liu, J., Weber, R.J. and Buseck, P.R.: Aerosol optical properties at Pasadena, CA during CalNex 2010, Atmos. Environ., 55, pp.190-200, doi:10.1016/j.atmosenv.2012.03.011, 2012.

Toon, G. C., Farmer, C. B., Schaper, P. W., Lowes, L. L., and Norton, R. H.: Composition measurements of the 1989 Arctic winter stratosphere by airborne infrared solar absorption spectroscopy, J. Geophys. Res., 97, 7939–7961, 1992.

Winker, D. M., Vaughan, M. A., Omar, A. H., Hu, Y., Powell, K. A., Liu, Z., Hunt, W. H., and Young, S. A.: Overview of the CALIPSO Mission and CALIOP Data Processing Algorithms, J. Atmos. Oceanic Technol., 26, 2310–2323, 2009

Wong, K. W., Fu, D., Pongetti, T. J., Newman, S., Kort, E. A., Duren, R., Hsu, Y.-K., Miller, C. E., Yung, Y. L., and Sander, S. P.: Mapping CH_4 : CO_2 ratios in Los Angeles with CLARS-FTS from Mount Wilson, California, Atmos. Chem. Phys., 15, 241–252, 2015.

Wong, K. W., Pongetti, T. J., Oda, T., Rao, P., Gurney, Kevin. R., Newman, S., Duren, R. M., Miller, C. E., Yung, Y. L., and Sander, S. P.: Monthly trends of methane emissions in Los Angeles from 2011 to 2015 inferred by CLARS-FTS observations, Atmos. Chem. Phys. Discuss., doi:10.5194/acp-2016-232, in review, 2016.

Wunch, D., Toon, G. C., Blavier, J.-F. L., Washenfelder, R., Notholt, J., Connor, B. J., Griffith, D. W. T., Sherlock, V., and Wennberg, P. O.: The Total Carbon Column Observing Network, Phil. Trans. R. Soc. A, 369, 2087–2112, doi:10.1098/rsta.2010.0240, 2011.

Xi, X., Natraj, V., Shia, R. L., Luo, M., Zhang, Q., Newman, S., Sander, S. P., and Yung, Y. L.: Simulated retrievals for the remote sensing of CO_2, CH_4, CO, and H_2O from geostationary orbit, Atmos. Meas. Tech., 8, 4817-4830, doi:10.5194/amt-8-4817-2015, 2015.

Yoshida, Y., Ota, Y., Eguchi, N., Kikuchi, N., Nobuta, K., Tran, H., Morino, I., and Yokota, T.: Retrieval algorithm for CO_2 and CH_4 column abundances from short-wavelength infrared spectral observations by the Greenhouse gases observing satellite, Atmos. Meas. Tech., 4, 717–734, doi:10.5194/amt-4-717-2011, 2011.

Zhang, Q., Natraj, V., Li, K.-F., Shia, R.-L., Fu, D., Pongetti, T. J., Sander, S. P., Roehl, C. M., and Yung, Y. L.: Accounting for aerosol scattering in the CLARS retrieval of column averaged CO_2 mixing ratios, J. Geophys. Res. Atmos., 120, doi:10.1002/2015JD023499, 2015.

Zhang, Q., Shia, R.-L., Sander, S. P., and Yung, Y. L.: XCO_2 retrieval error over deserts near critical surface albedo, Earth Space Sci., 2, doi:10.1002/2015EA000143, 2016.

Atmos. Chem. Phys. Discuss., doi:10.5194/acp-2016-490, 2016
Manuscript under review for journal Atmos. Chem. Phys.
Published: 20 June 2016

Atmospheric Chemistry and Physics Discussions

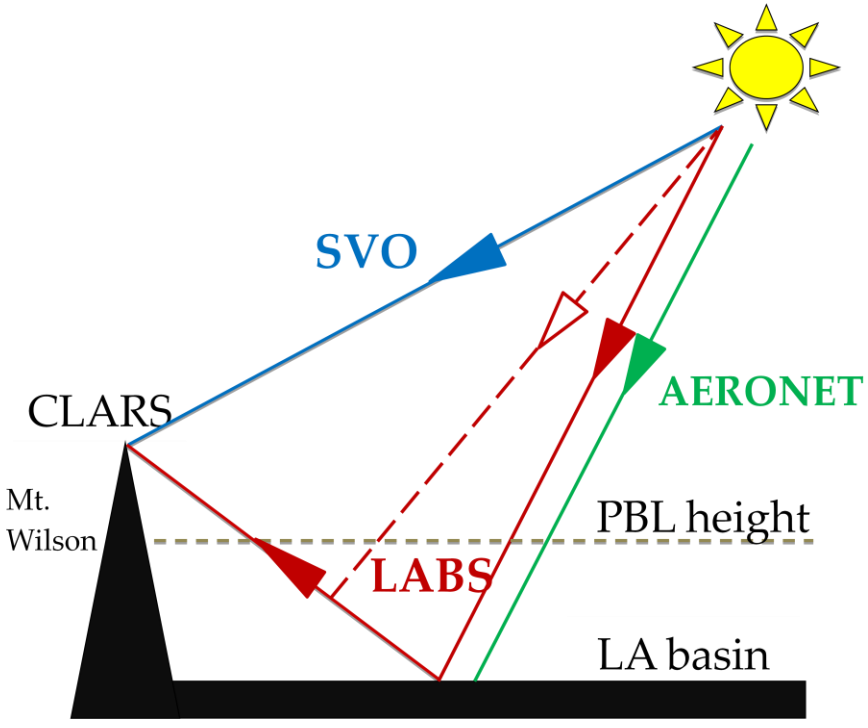

Figure 1. Schematic diagram of CLARS-FTS measurement geometries for West Pasadena and the AERONET site at Caltech. CLARS-FTS has two modes of operation, including Los Angeles Basin Survey mode (LABS; in solid red) and the Spectralon Viewing Observation mode (SVO; in blue). An example of light path change due to aerosol scattering along the path from the basin to the mountain top is illustrated (in dotted red). Also shown is the light path of AERONET-Caltech (in green).

Atmos. Chem. Phys. Discuss., doi:10.5194/acp-2016-490, 2016
Manuscript under review for journal Atmos. Chem. Phys.
Published: 20 June 2016

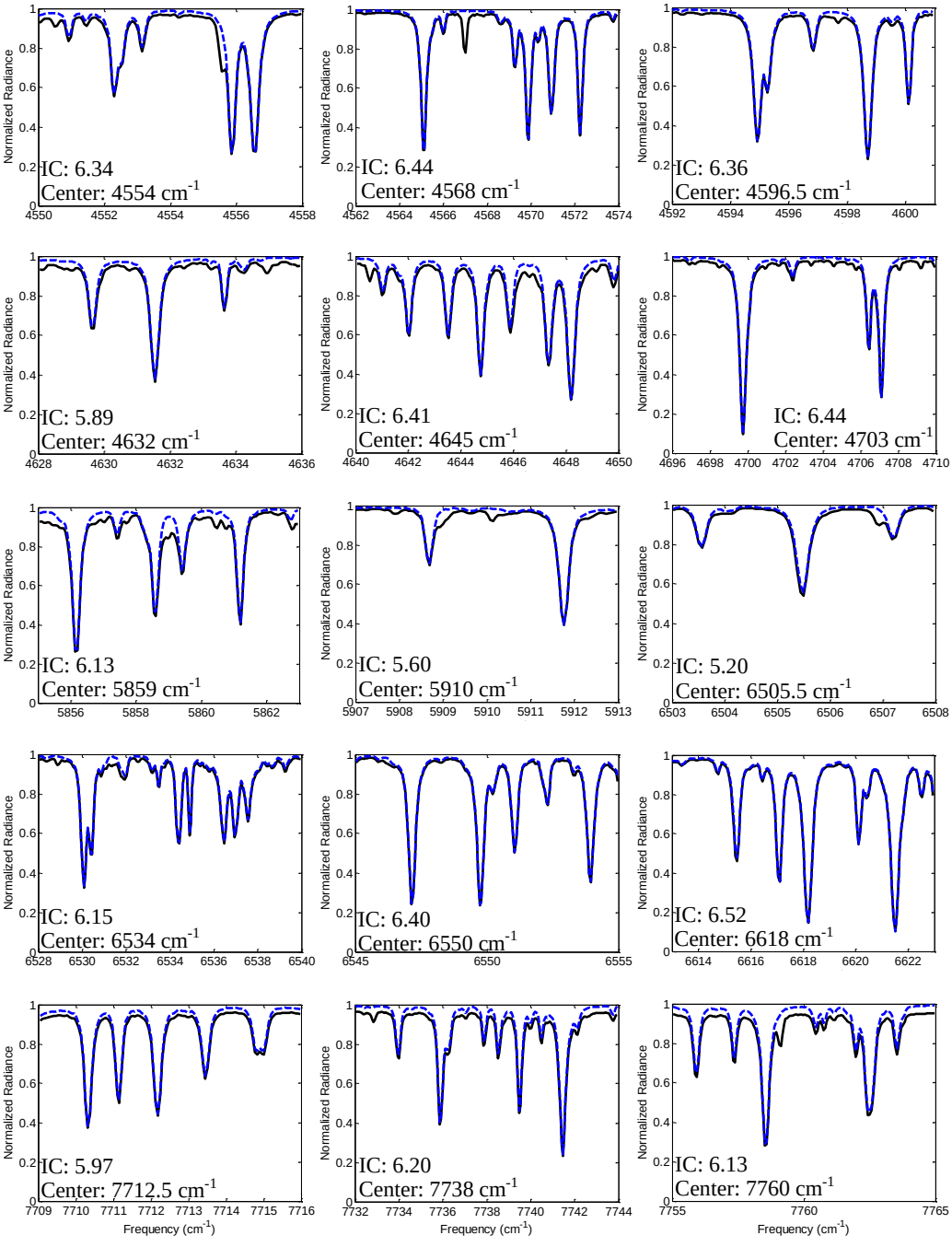

Figure 2. The normalized radiances of the 15 H_2O absorption bands selected for retrieving H_2O SCDs from CLARS-FTS measurements. These radiances are spectral fits using the CLARS-FTS measurements in West Pasadena on March 01, 2013 with a solar zenith angle (SZA) of 41.45 °. Solid black curves are fits to the spectra, including contributions of all trace gases and solar lines, from spectral measurements by the FTS and dashed blue curves are the estimated contribution of H_2O absorption to the spectral fits. Contributions of other species in these spectral regions are not shown. Wavelength of the center and information content (IC) value of each band for retrieving H_2O content are also given.

Atmos. Chem. Phys. Discuss., doi:10.5194/acp-2016-490, 2016
Manuscript under review for journal Atmos. Chem. Phys.
Published: 20 June 2016

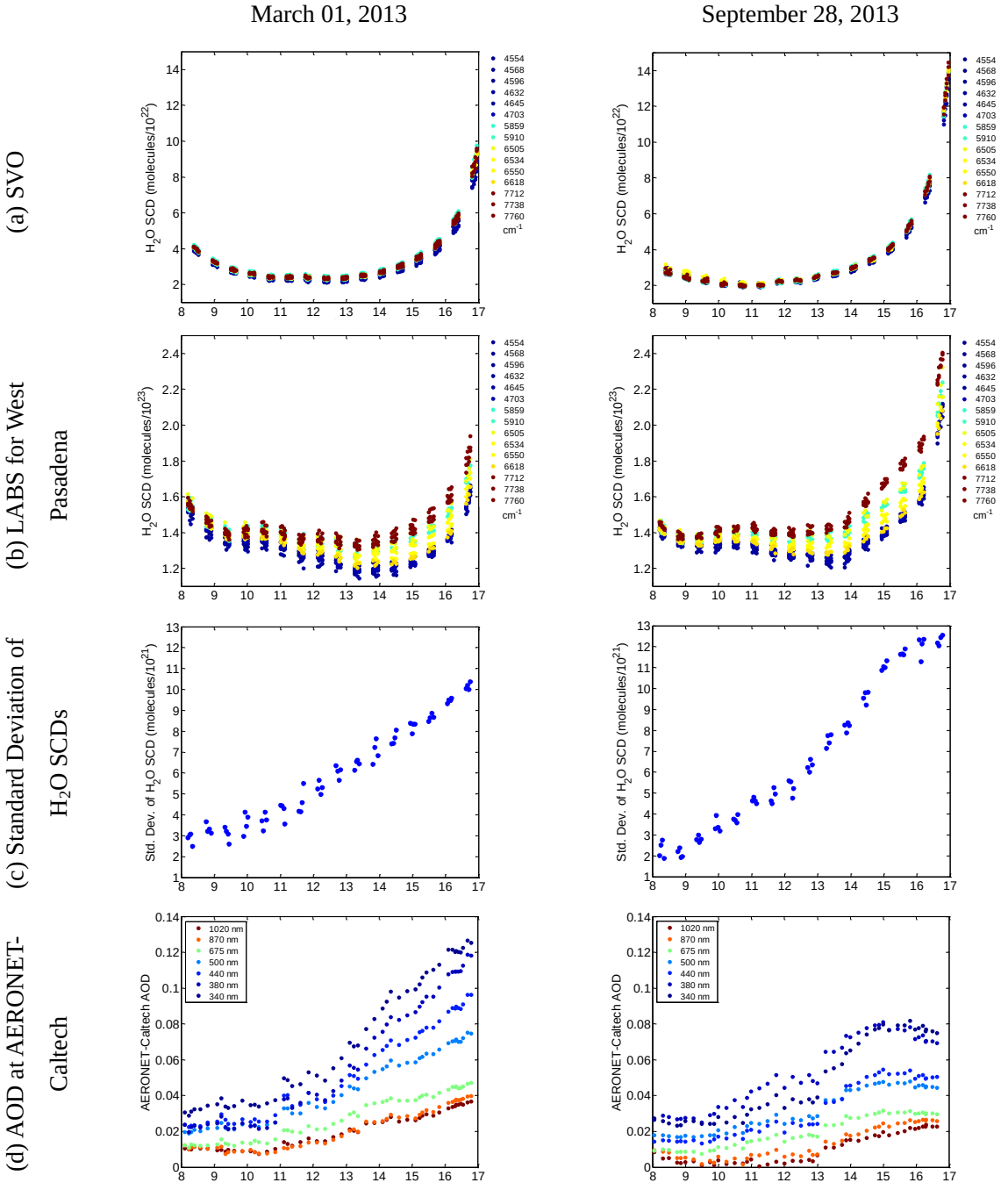

Figure 3. Daily Variations of CLARS H_2O SCD retrievals for the West Pasadena target and AOD measurements from AERONET-Caltech station on March 01, 2013 (left column) and September 28, 2013 (right column). H_2O SCD retrievals from SVO mode are shown in panel (a), and from LABS mode for West Pasadena are shown in panel (b). The corresponding standard deviations of H_2O SCD retrievals, a measure of the degree of variation in the retrievals, are shown in panel (c) and the AOD measurements from AERONET-Caltech are shown in panel (d).

Atmos. Chem. Phys. Discuss., doi:10.5194/acp-2016-490, 2016
Manuscript under review for journal Atmos. Chem. Phys.
Published: 20 June 2016

Atmospheric Chemistry and Physics Discussions

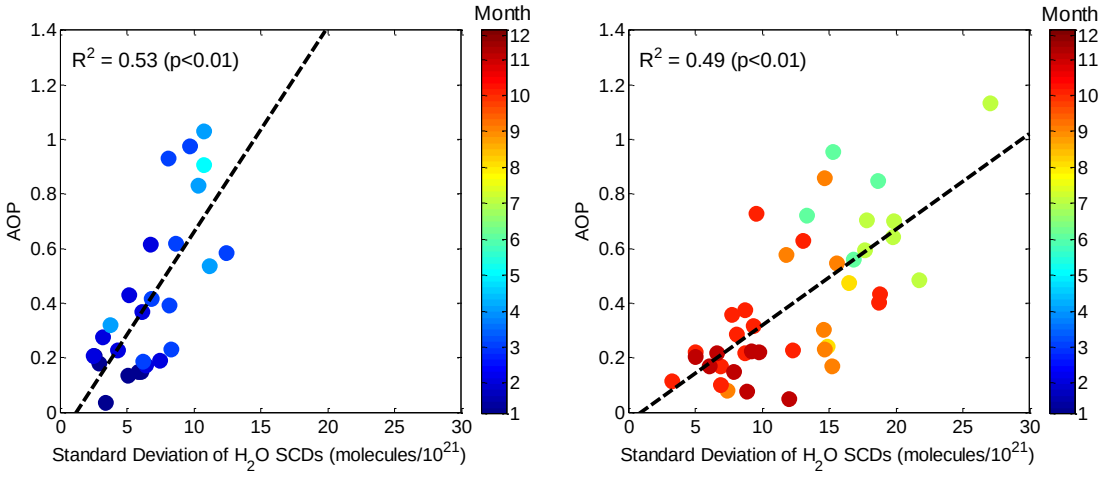

Figure 4. Correlation between daily averaged standard deviation of H_2O SCDs, a measure of retrieval differences, from 12:00 to 14:00 and the corresponding averaged AOP, calculated by scaling AOD data (1020 nm) from AERONET based on CLARS geometry, for two time periods in 2013. (a) Winter and spring, including January to May, in which the coefficient of determination (R^2) is 0.53 and [slope, intercept] = [0.08±0.03, -0.09±0.21] with 95% confidence bounds from linear regression. No December data from AERONET are available in 2013. (b) Summer and autumn from June to November, in which R^2 is 0.49 and [slope, intercept] = [0.04±0.01, -0.03±0.16]. In total, there are 67 days of daily mean data available in 2013, in which 27 days are for winter-spring and 40 days are for summer-autumn.

Atmos. Chem. Phys. Discuss., doi:10.5194/acp-2016-490, 2016
Manuscript under review for journal Atmos. Chem. Phys.
Published: 20 June 2016

Atmospheric Chemistry and Physics Discussions

(a)

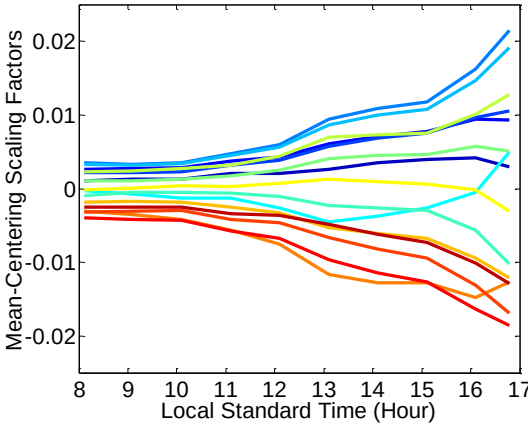

(b)

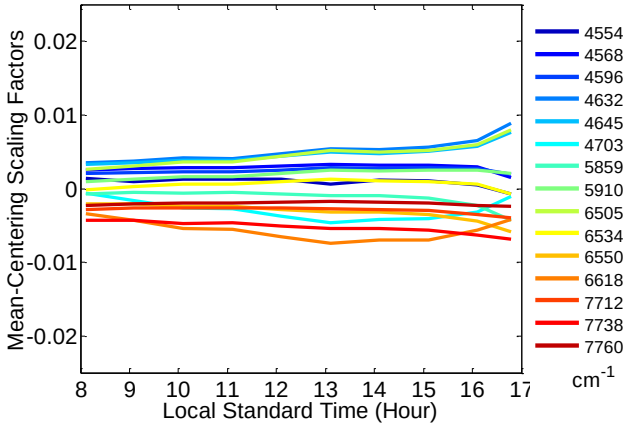

(c)

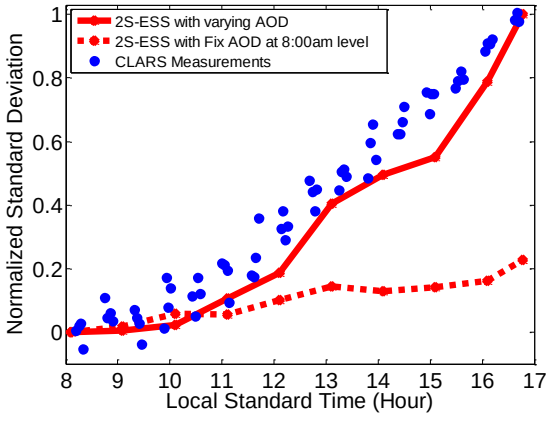

Figure 5. (a) Scaling factors for H_2O SCDs retrieved from the simulated synthetic spectral radiance of the 15 chosen bands using 2S-ESS RT model with AOD data from AERONET-Caltech on March 01, 2013. The scaling factors are mean-centered by subtracting the mean to clearly show the variations in the retrievals; (b) The same as (a) except that the AOD is fixed at the 8:00 level for all hours across the day; (c) Comparison between CLARS measurements and results from the two RT model experiments in (a) and (b) in terms of standard deviations, a measure of variations in H_2O SCDs retrieved from the 15 chosen bands. The standard deviations are normalized to be between 0 and 1 for both measurements and simulations. When normalizing, the half-hourly mean of the CLARS data is calculated to obtain the maximum and minimum for the normalization.